

Supplementary Material

Curcumin-Based Pyrazoline Analogues as Selective Inhibitors of Human Monoamine Oxidase A

Chandrani Nath¹, Vishnu N. Badavath¹, Abhishek Thakur³, Gulberk Ucar^{*,2}, Orlando Acevedo^{*,3}, Mohd Usman Mohd Siddique¹, Venkatesan Jayaprakash^{*,1}

¹Department of Pharmaceutical Sciences & Technology, Birla Institute of Technology, Mesra, Ranchi-835 215, Jharkhand, India

²Department of Biochemistry, Faculty of Pharmacy, Hacettepe University, Sıhhiye 06100, Ankara, Turkey

³Department of Chemistry, University of Miami, Coral Gables, Florida 33146, USA

1. Chemistry

Materials and Methods: All the chemicals and solvents for synthesis were purchased from Aldrich. Unless otherwise mentioned the solvents were used without purification. Reactions were monitored by TLC on precoated silica gel plates (Kieselgel 60 F 254, Merck) and the spots were detected under UV light (254 nm). Purification was performed by column chromatography using silica gel (particle size 100-200 mesh, CDH). Melting points were determined using Optimelt (Stanford Research Systems, Sunnyvale, CA 94089) by capillary method and are uncorrected. Specific rotation of the compounds were determined using Automatic Polarimeter A21102 API/1W, serial No.: 3.485 (Rudolf Research Analytical, USA). Infrared (IR) spectra were taken on a FT-IR Spectrophotometer IR-Prestige 21 (Shimadzu Corporation, Japan) from 4000-400 cm⁻¹ using KBr discs. ¹H-NMR spectra were recorded on Varian 400 MHz instrument in DMSO-*d*₆ as a solvent. Chemical shifts are reported in parts per million (δ) downfield with respect to tetramethylsilane (TMS, δ= 0.0) as internal standard. Spin multiplicities are given as s (singlet), d (doublet), t (triplet), and m (multiplet) as well as b (broad). Coupling constants (*J*) are given in hertz. Mass spectra were recorded by the ESI-MS Electro spray Ionization technique. Chiral separation of the compounds were achieved using analytical chiral column CHIRALPAK 1A (250x4.6mm, 5μ) in 1260 Infinity II LC system (Agilent) with PDA detector.

Synthetic procedure for the synthesis of 4-(5-(4-chlorophenyl)-4,5-dihydro-1H-pyrazol-3-yl)-2-methoxyphenol (2)

Chalcone **1** (2gm) was treated with hydrazine hydrate (10mL) in ethanol (50mL) and refluxed for 3-6 h. Then the hot reaction mixture was poured into ice-cold water. The solid separated out was filtered, washed with water, dried and recrystallized from ethanol to afford desired compound. Yield: 85%; mp: 79-81 °C; [α]_D^{30.2} = -9.688°; ¹H-NMR (400MHz, DMSO-*d*₆): δ (ppm) 2.716-2.782 (H_A, dd, J_{AM}=16Hz, J_{AX}=10.4Hz), 3.356-3.423 (H_M, dd, 1H, J_{MA}=16.4Hz, J_{MX}=10Hz), 3.767 (s, 3H, -OCH₃), 4.739-4.775 (H_X, dd, J_{XM}=10.8Hz, J_{XA}=3.6Hz), 6.738-6.757 (d, 1H, Ar-H, J=7.6Hz), 6.944-6.940 (d, 2H, Ar-H, J=6.4Hz), 7.214 (s, 1H, Ar-H), 7.303-7.311 (d, 1H, Ar-H, J=3.2Hz), 7.379 (s, 4H, Ar-H, merged dd of Ring B protons), 9.23 (s, broad peak, Ar-OH); ESI-MS (m/z): Calculated 302.08, observed 303 [M+1]⁺

*Synthetic procedure for the synthesis of (5-(4-chlorophenyl)-3-(4-hydroxy-3-methoxyphenyl)-4,5-dihydro-1H-pyrazol-1-yl)(phenyl)methanone (3)*¹

To the pyrazoline **2** (0.001M) in pyridine (10mL), benzoyl chloride (0.002M) was added. The reaction mixture was heated on water bath for 3-4 h and poured over crushed ice mixed with dilute hydrochloric acid. The solid separated out was filtered, washed with water, dried and recrystallized from ethanol to afford desired compound. Yield: 85%; mp: 50-53 °C; [α]_D^{30.5} = -5.51°; ¹H-NMR (400MHz, DMSO-*d*₆): δ (ppm) 3.123-3.872 (H_A, dd, J_{AM}=17.6Hz, J_{AX}=4.4Hz), 3.756 (s, 3H, -OCH₃), 3.733-3.872 (H_M, dd, 1H, J_{MA}=14.8Hz, J_{MX}=8.8Hz), 5.710-5.749 (H_X, dd, J_{XM}=11.2 Hz, J_{XA}=4.4 Hz), 6.812-6.833 (d, 1H, Ar-

\underline{H} , $J=4.8$ Hz), 7.146-7.167 (d, 1H, Ar- \underline{H} , $J=8.4$), 7.216 (s, 1H, Ar- \underline{H}), 7.288-7.309 (d, 1H, Ar- \underline{H} , $J=8.4$ Hz), 7.385-7.406 (d, 1H, Ar- \underline{H} , $J=8.4$ Hz), 7.459-7.491 (t, 3H, Ar- \underline{H}), 7.585-7.599 (d, 1H, Ar- \underline{H} , $J=5.6$ Hz), 7.866-8.940 (dd, 4H, Ar- \underline{H} , Ring B protons), 9.59 (s, 1H, Ar-OH); ESI-MS (m/z): Calculated 406.86, observed 407.0 $[M+1]^+$

Synthetic procedure for the synthesis of 4-(5-(4-chlorophenyl)-1-tosyl-4,5-dihydro-1H-pyrazol-3-yl)-2-methoxyphenol (4)¹

p-Toluene sulphonyl chloride (0.0025) was dissolved in tetrahydrofuran (2 mL) with stirring. The stirred mixture was cooled in an ice bath to 10-15 °C; followed by gradual addition of a solution of pyrazoine 2 in tetrahydrofuran so that the temperature was maintained between 10-15 °C. Stirring was continued for 10-15 min. after the addition was complete. The solid separated out was filtered, dried and recrystallized from methanol to afford desired compound. Yield: 70 %; mp: 216-218 °C; $[\alpha]_D^{30.6} = -6.468^\circ$; $^1\text{H-NMR}$ (400MHz, DMSO- d_6): δ (ppm) 2.226 (s, 3H, Ar- $\underline{CH_3}$), 3.507-3.572 (H_A , dd, 1H, $J_{AM}=18$ Hz, $J_{AX}=8.8$ Hz), 3.790-3.857 (m, 4H, merged peak -OCH $\underline{3}$ and H_M proton), 5.167 (t, H_M 1H, merged peak), 6.88 (d, 1H, Ar-H), 7.09 (d, 2H, Ar-H), 7.299 (d, 1H, Ar-H), 7.385 (s, 1H, Ar-H), 7.444-7.521 (m, 6H, Ar-H), 9.95 (bs, 1H, Ar-OH); ESI-MS (m/z): Calculated 456.94, observed 457.1 $[M+1]^+$; $^{13}\text{C-NMR}$ (100 MHz, DMSO- d_6): δ (ppm) 21.23 (Ar-CH $\underline{3}$), 41.38 (pyr-C4), 56.16 (Ar-OCH $\underline{3}$), 60.78 (pyr-C5), 111.43, 115.97, 120.57, 123.32, 125.93, 128.56, 129.32, 130.31, 134.18, 134.89, 138.28, 145.79, 148.28, 151.41 (pyr-C3).

Synthetic procedure for the synthesis of 5-(4-chlorophenyl)-3-(4-hydroxy-3-methoxyphenyl)-N-phenyl-4,5-dihydro-1H-pyrazole-1-carbothioamide (5)²

To the stirred solution of pyrazoine 2 (0.001M.) in absolute ethanol, was added phenyl isothiocyanate (0.002M.) and refluxed for 2-3 h. The obtained crude precipitate of product was filtered, washed with petroleum ether, dried, and was recrystallized from methanol. Yield: 90%; mp: 160 °C; $[\alpha]_D^{30.5} = -5.517^\circ$; $^1\text{H-NMR}$ (400MHz, DMSO- d_6): δ (ppm) 3.149-3.203 (H_A , dd, $J_{AM}=18$ Hz, $J_{AX}=3.6$ Hz), 3.834 (s, 3H, -OCH $\underline{3}$), 3.852-3.926 (H_M , dd, 1H, $J_{MA}=18.4$ Hz, $J_{MX}=11.2$ Hz), 5.971-6.006 (H_X , dd, $J_{XM}=11.2$ Hz, $J_{XA}=3.6$ Hz), 6.804-6.825 (d, 1H, Ar- \underline{H} , $J=8.4$ Hz), 7.132-7.204 (m, 3H, Ar- \underline{H}), 7.272-7.343 (m, 3H, Ar- \underline{H}), 7.368-7.388 (d, 2H, Ar- \underline{H} , $J=8$ Hz), 7.516-7.535 (d, 2H, Ar- \underline{H} , $J=7.6$ Hz), 7.6 (s, 1H, Ar- \underline{H}), 9.644 (s, 1H, Ar-OH), 10.042 (s, 1H, -NH-); ESI-MS (m/z): Calculated 437.94, observed 438 $[M+1]^+$

Synthetic procedure for the synthesis of phenyl 5-(4-chlorophenyl)-3-(4-hydroxy-3-methoxyphenyl)-4,5-dihydro-1H-pyrazole-1-carboxylate (6)³

To the solution of pyrazoine 2 (0.001M) in ethanol (10 mL), was added an equimolar quantity of phenylchloroformate (0.002M) drop-wise at <10 °C with stirring. An equimolar quantity of potassium carbonate was added and stirring continued for another 30 min. The reaction mixture was then filtered and the filtrate upon evaporation provided desired compound. Yield: 70%; mp: 160-163 °C; $[\alpha]_D^{30.5} = -7.23^\circ$; $^1\text{H-NMR}$ (400MHz, DMSO- d_6): δ (ppm) 3.150-3.224 (H_A , dd, $J_{AM}=16.4$ Hz, $J_{AX}=12$ Hz), 3.759 (s, 3H, -OCH $\underline{3}$), 3.822-3.896 (H_M , dd, 1H, $J_{MA}=18$ Hz, $J_{MX}=11.6$ Hz), 5.5 (bs, 1H, H_X protons merged peak), 6.717-6.738 (d, 1H, Ar- \underline{H} , $J=8.4$ Hz), 7.084-7.104 (d, 2H, Ar- \underline{H}), 7.103-7.20 (m, 2H, Ar- \underline{H}), 7.258 (t, 2H, Ar- \underline{H}), 7.406-7.426 (d, 2H, Ar- \underline{H} , $J=8$ Hz); ESI-MS (m/z): Calculated 422.86, observed 423 $[M+1]^+$

1.1. Specific rotation:

Compounds 2-6, in 5 mg quantity were dissolved in HPLC grade methanol. Sample solutions were then measured for specific rotation at λ 589 nm (sodium D line) using sample cell having 10 cm path-length.

1.2. Chiral separation using analytical chiral column:

Chiral separation of the compounds were achieved using analytical chiral column CHIRALPAK 1 A (250 x 4.4 mm, 5 μ) with sample injection volume of 20 μ L, mobile phase (5-10% isopropyl alcohol in n-hexane) flow rate of 1.0 mL/min. Detection was done at λ 210 nm. The data obtained is presented in Table S1.

Table S1. Chiral separation of compounds 2-6

Code	Mobile phase	Retention time (min)		% area	
		Peak 1	Peak 2	Peak 1	Peak 2
2	5% isopropyl alcohol in n-hexane	9.235	11.112	49.996	50.006
3	10% isopropyl alcohol in n-hexane	10.599	15.154	97.966	2.034
4	10% isopropyl alcohol in n-hexane	9.971	11.640	1.164	98.836
5	10% isopropyl alcohol in n-hexane	15.090	17.789	98.842	1.158
6	5% isopropyl alcohol in n-hexane	7.107	11.348	4.779	93.550

2. Biochemistry

MAO activity screening: All the compounds were screened for their *h*MAO inhibitory activity using Amplex®-Red MAO assay Recombinant enzymes and chemicals were according to the manufacturer's instructions. The assay is a one-step fluorometric method for the continuous measurement of MAO activity using a fluorescence microplate reader. The assay is based on the detection of H₂O₂ in a horseradish peroxidase coupled reaction using Amplex Red reagent, a highly sensitive and stable probe for H₂O₂. The reaction product, resorufin, is highly stable. No interference from autofluorescence was detected in the biological samples in our studies since resorufin has absorption and fluorescence emission maxima of 571 nm and 585 nm. *p*-tyramine (0.05-0.50 mM) was used as the common substrate for both *h*MAO-A and -B. Specific inhibitors of *h*MAO-A and -B were used for the determination of these *h*MAO isoforms.

Recombinant enzymes were diluted in a reaction buffer (containing 0.25 M of sodium phosphate, pH 7.4). 100 μ L enzyme solution was used for each reaction. One of the MAO-inhibitors was included, by adding the equivalent of 0.2 μ L of the 0.5 mM inhibitor stock solution (clorgyline or pargyline) to each 100 μ L volume of diluted sample and the samples were preincubated at room temperature for 30 min. Enzyme and inhibitor concentrations were kept as two-fold lower in the final reaction volume. The positive control solution was prepared by diluting the 20 mM H₂O₂ working solution to the final concentration of 10 μ M in reaction buffer whereas the action buffer without H₂O₂ was prepared as the negative control.

Reaction was started by adding 100 μ L of the Amplex Red reagent (400 /HRP/substrate working solution) to each microplate well containing the samples and controls. Mixtures were incubated for 30 min at room temperature. Fluorescence was measured using excitation at 530 nm and emission at 590 nm at multiple time points to follow the kinetics of the reactions. Background fluorescence was corrected by subtracting the values derived from then *o*-amine oxidase control. The possible capacity of the new compounds to modify the fluorescence generated in the reaction mixture due to non-enzymatic inhibition was determined by adding these compounds to solutions containing only the Amplex Red reagent in a

sodium phosphate buffer. Newly synthesized compounds did not cause any inhibition on the activity of HRP in the test medium.

Specific enzyme activities were calculated as 0.151 ± 0.007 nmol/mg/min (n=3) for *h*MAO-A and 0.133 ± 0.009 nmol/mg/min (n=3) for *h*MAO-B.

Kinetic studies

Synthesized compounds were dissolved in dimethyl sulfoxide (DMSO), with a maximum concentration of 1% and used in a concentration range of 0.01 μ M-6.00 mM. Selegiline, moclobemide and lazabemide were dissolved also in DMSO in a concentration range of 0.01 μ M-10 mM. The mode of *h*MAO inhibition was examined using Lineweaver-Burk plotting (refer to Figure 2 in Manuscript). The slopes of the Lineweaver-Burk plots were plotted versus the inhibitor concentration and the inhibitor constant (K_i) values were determined from the x-axis intercept as $-K_i$. Each K_i value is the representative of single determination where the correlation coefficient (R^2) of the replot of the slopes versus the inhibitor concentrations was at least 0.98. SI was calculated as $K_i(h\text{MAO-B})/K_i(h\text{MAO-A})$. The protein was determined according to the Bradford method.⁴

Reversibility

Reversibility of the *h*MAO inhibition with the compounds was determined by dialysis method previously described.⁵ Briefly, dialysis tubing of 16x25 mm with a molecular weight cut-off of 12,000 and a sample capacity of 0.5-10 mL was used. Recombinant enzymes were incubated with the compounds a concentration as fivefold of the K_i values for the inhibition of *h*MAO-A and -B, respectively in potassium phosphate buffer (0.05 M, pH 7.4, 5% sucrose containing 1% DMSO) for 15 min. at 37 °C. Other sets were prepared by preincubation of same amount of *h*MAO-A and -B with the reference inhibitors. Enzyme-inhibitor mixtures were subsequently dialyzed at 4°C in dialysis buffer (100 mM potassium phosphate, pH 7.4, 5% sucrose). The dialysis was repeated two times during the 24 h of dialysis. After dialysis, residual MAO activities were measured (*p*-tyramine was used as substrate at 0.10 mM). All reactions were carried out in triplicate and the residual enzyme activity was expressed as mean \pm SEM (Table S2). For comparison, undialyzed mixtures of the MAOs and the inhibitors were included in the study.

Table S2. Reversibility of the inhibition of *h*MAO isoforms by compounds

Compounds incubated with <i>h</i> MAO	<i>h</i> MAO-A activity before washing (%)	<i>h</i> MAO-A activity after washing (%)	<i>h</i> MAO-B activity before washing (%)	<i>h</i> MAO-B activity after washing (%)	Reversibility
2	39.45 \pm 1.08	94.20 \pm 2.55	90.12 \pm 4.13	98.00 \pm 1.24	Reversible
3	71.00 \pm 1.65	94.50 \pm 2.27	93.10 \pm 2.80	96.27 \pm 2.76	Reversible
4	70.11 \pm 2.55	91.76 \pm 2.88	91.00 \pm 2.46	94.80 \pm 3.04	Reversible
5	80.80 \pm 2.00	94.16 \pm 1.98	90.50 \pm 1.75	93.22 \pm 1.08	Reversible
6	77.24 \pm 2.16	89.45 \pm 2.11	88.10 \pm 1.75	92.72 \pm 2.71	Reversible
Moc	33.01 \pm 2.03	96.28 \pm 2.55	84.00 \pm 2.16	95.22 \pm 3.55	Reversible
Sel	89.95 \pm 2.48	92.00 \pm 3.24	51.55 \pm 3.22	50.60 \pm 1.98	Irreversible
Laz	90.12 \pm 2.17	94.45 \pm 3.70	12.00 \pm 1.01	93.44 \pm 3.77	Reversible
Ctrl	100 \pm 0.00	100 \pm 0.00	100 \pm 0.00	100 \pm 0.00	-

*Each value represents the mean \pm SEM (n=3). Sel: Selegiline; Laz: Lazabemide; Moc: Moclobemide; Ctrl: Without Inhibitor

Cytotoxicity Studies

Cell viability was measured by a quantitative colorimetric assay with 3-[4,5 dimethylthiazol-2-yl]-2,5-diphenyl-tetrazolium bromide (MTT) (Sigma Aldrich).⁶ Human hepatoma cell line HepG2 (Invitrogen) was cultured in Dulbecco's Modified Eagle's Medium (DMEM) supplemented with 2 mM L-Glutamine, 10% heat-inactivated fetal bovine serum (FBS), 100 units/mL penicillin, and 100 µg/mL streptomycin. Cells were seeded in supplemented medium and maintained at 37°C in a humidified atmosphere of 5% CO₂ and 95% air. Exponentially growing HepG2 cells were subcultured in 96-well plates. The cells were treated with the compounds at the concentrations of 1, 5 and 25 µM, and 0.1% DMSO as a vehicle control for 24 h. 10 µL of the MTT labeling reagent, at a final concentration of 5 mg/mL, was added to each well at the end of the incubation time and the plate placed in a humidified incubator at 37°C with 5% CO₂ and 95% air (v/v) for 4 h until the appearance of purple formazan crystals formed. Then, the insoluble formazan was dissolved with 100 µL of dimethylsulfoxide (DMSO) by shaking 1 h in darkness. MTT reduction was measured at 590 nm. Control cells treated with 0.1% DMSO were used as 100% viability.⁷ Significance was determined using student's t-test. Results were expressed as mean±SEM. Differences are considered statistically significant at p<0.05.

***In vitro* blood–brain barrier permeation assay (PAMPA-BBB):**

The penetration of newly synthesized compounds into brain was determined using parallel artificial membrane permeation assay (PAMPA) for blood–brain-barrier according to a previous method.⁸ Briefly, compounds and the commercial drugs were dissolved in DMSO at a concentration of 5 mg/mL. They were diluted with a mixture of PBS/EtOH (70:30) to give a final concentration of 25 µg/mL. The filter membrane in donor microplate was coated with porcine polar brain lipid (PBL) dissolved in dodecane (4 µL, 20 mg/mL). 200 µL of diluted solution and 300 µL of PBS/EtOH (70:30) were added to the donor and the acceptor wells, respectively. The donor filter plate was carefully placed on the acceptor plate. Sandwich system was kept at 250 °C for 16 h. The donor plate was carefully removed, and the concentrations of the compounds and the commercial drugs in the acceptor, donor and reference wells were measured with a UV plate reader.

Molecular modeling simulation

Molecular Docking Simulation Protocol.

Docking studies were performed using the AutoDock4.2 program, which combines the Lamarckian Genetic Algorithm with an empirical force field to yield fast predictions of binding modes and energies. Relative errors of 2-3 kcal/mol are typical per conformation. Determining the correct binding site of human monoamine oxidase A (*h*MAO-A) co-crystallized with harmine (HRM) [PDB ID: 2Z5X] was the initial priority.⁹ AutoGridFR (AGFR) was used to compute the binding affinity over the entire receptor by scoring different binding pockets based on AutoSite (AS) results.¹⁰ The AS score for the HRM binding site (colored in green in Figure S1) yielded the most favorable result. Interestingly, two additional regions, shown colored in orange and yellow in Figure S1, were found adjacent to the flavin adenine dinucleotide (FAD) binding site that gave comparable AS scores. In order to cross check the predicted binding pockets, a separate program AutoLigand was used to calculate the binding affinity values at the HRM receptor site and to independently evaluate the alternative binding pockets.¹¹ Default protocol affinity maps were calculated for the receptor with grid size of 40 Å along the *x*, *y* and *z* axis with the grid centered on the receptor. Autoligand also predicted the highest binding affinity to be located at co-crystallized HRM site (Figure S2). Thus, the calculations suggest that any *de novo* designed ligands should target the HRM binding site.

Based on results from AGFR and AutoLigand, a grid was centered over the HRM binding region with a box size set at *x* = *y* = *z* = 30 grid points. Protein preparation was carried out by removing all crystallographic water molecules, adding polar hydrogens, computing Kollman charges, and assigning atomic radii and AutoDock4 atomtypes. Docking parameters were created using default values except the

exhaustiveness of the global search was set to 100 and docking parameters were saved in DPF format. The co-crystallized HRM ligand was removed and re-docked using the prescribed method above and the binding mode was accurately reproduced (Figure S3). After validating the docking method, the 2*R*, 2*S*, 4**R* and 4**S* were docked. The docking poses obtained for the 2*R* and 2*S* conformers had similar orientations compared to HRM in the receptor site. For example, the keto groups of *R*, *S*, and HRM compounds were oriented in same general direction within the active site (Figure S4). Complexes of all the four ligands with *h*MAO-A were prepared for further molecular dynamics simulations.

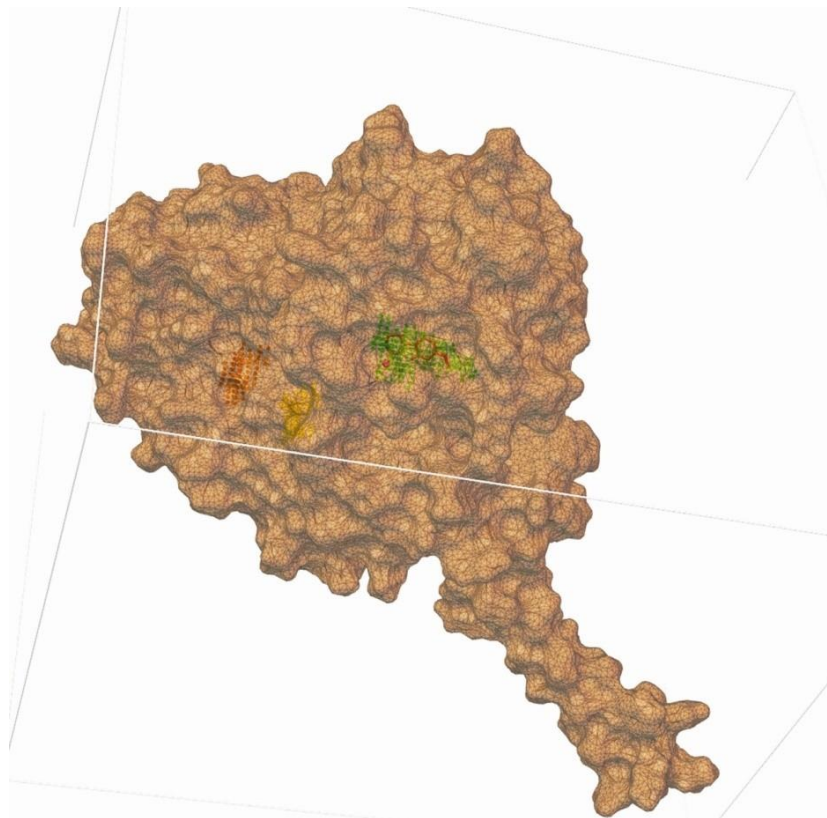


Figure S1. Space-filling representation of *h*MAO-A [PDB ID:2Z5X]. AutoGridFR calculations predicted the best score corresponded to the HRM binding site (green region). Two additional potential binding sites were identified and colored here as orange and yellow.

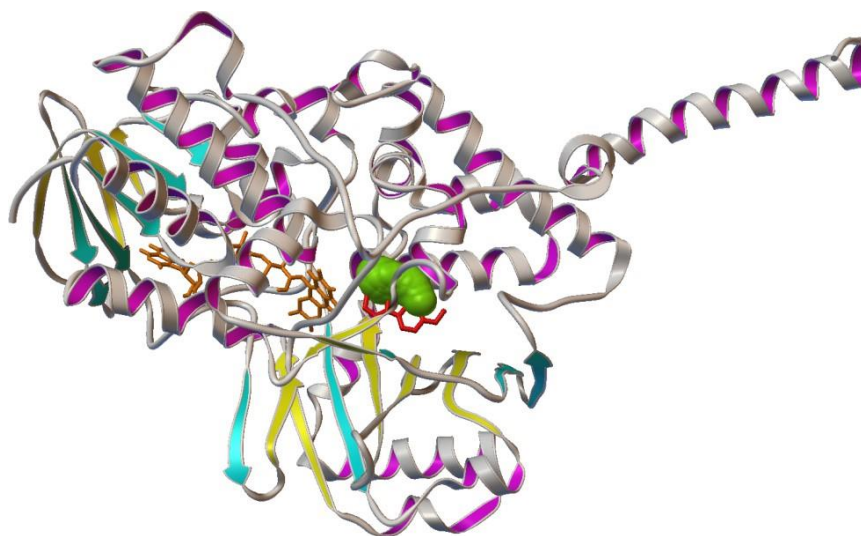


Figure S2. Autoligand predicted the binding site (shown in green) to be near the crystallographic HRM binding site (shown in red) and adjacent to FAD (given in orange).

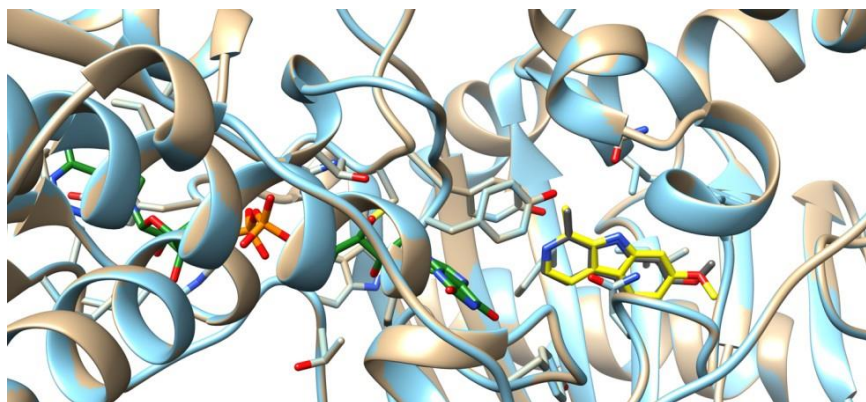


Figure S3. A comparison of HRM binding modes from the co-crystallized 2Z5X structure (grey) and AutoDock4 (yellow).

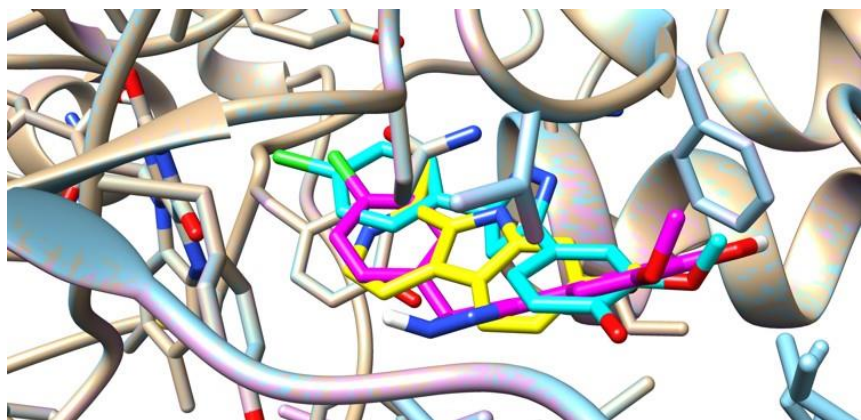


Figure S4. A superimposed image of HRM (yellow), 2R (pink) and 2S (cyan) bound to *h*MAO-A.

Molecular Mechanics/Poisson-Boltzmann Surface Area.

MM/PBSA (molecular mechanics/Poisson-Boltzmann surface area) calculations¹² were carried out to compute the free energies of binding (ΔG_{bind}) for the different ligands in complex with *h*MAO-A. The dielectric constant for the interior of the protein was set to 1 and an implicit solvent model was used with a dielectric of 80. The free energy calculation utilized the 100 ns trajectories from the production runs; however, entropic contributions were not included.

BIT2015-001 in DMSO-d6
A.R.No : NE15D013

Sample Name:

Data Collected on:

DRILS-vnmrs400

Archive directory:

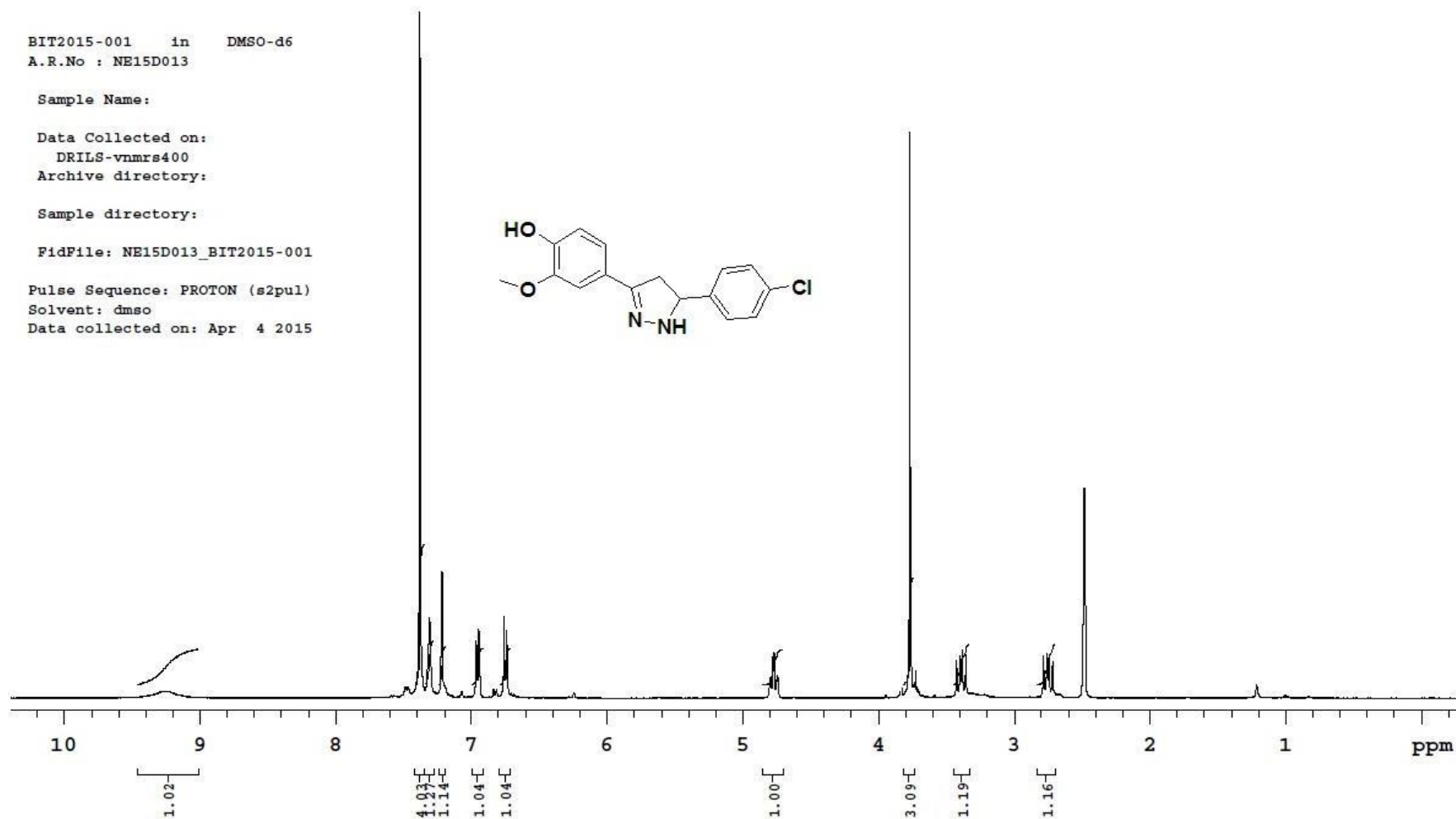
Sample directory:

FidFile: NE15D013_BIT2015-001

Pulse Sequence: PROTON (s2pul)

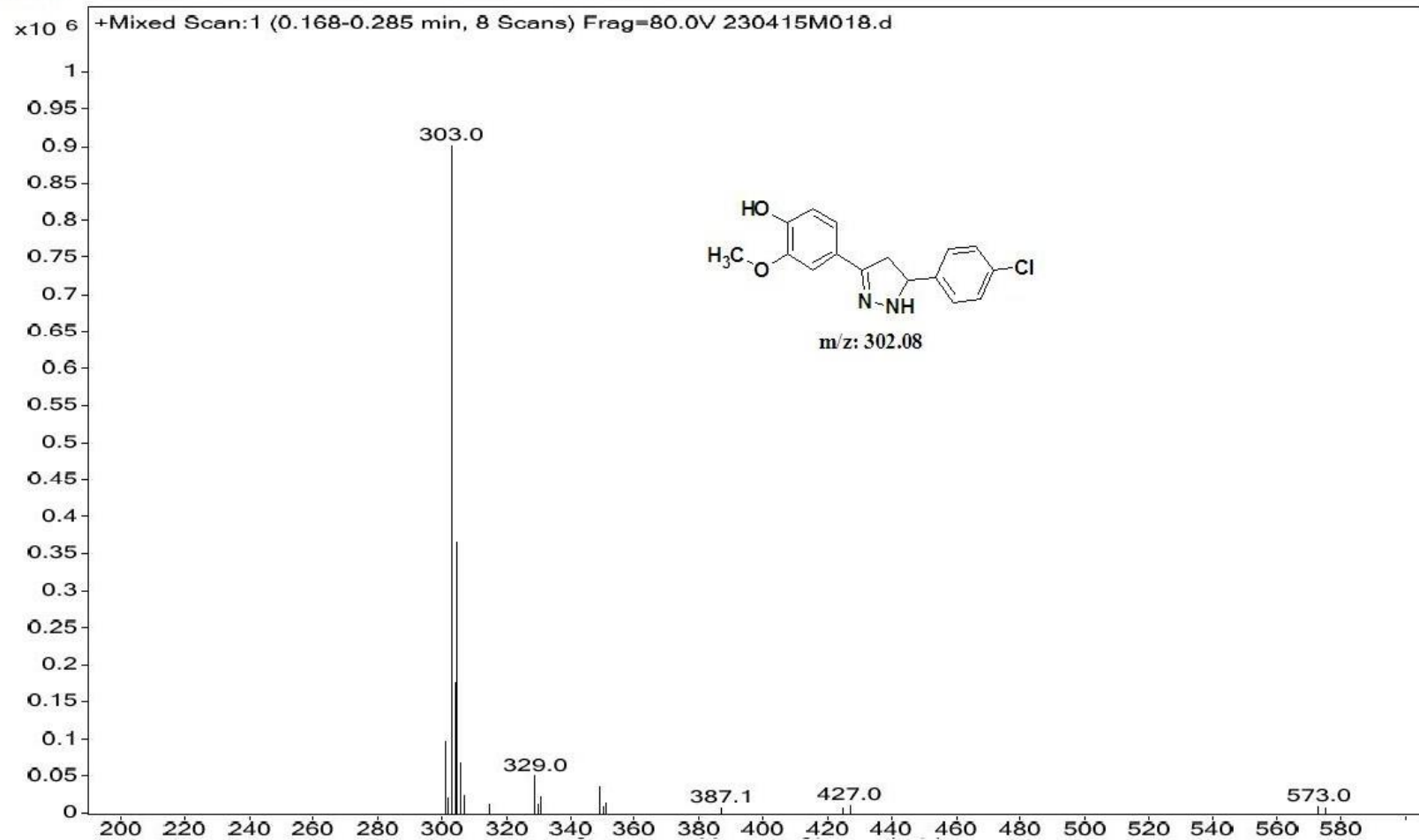
Solvent: dmsd

Data collected on: Apr 4 2015



¹H-NMR (400 MHz, DMSO-d₆) spectrum of compound 2

Sample Name	BIT2015-001	Position	Vial 18	Sample type		Instrument Name	Instrument 1
User Name		Inj Vol	0.5	Data Filename	230415M018.d	ACQ Method	test.m
AR NO :	ME15D095	Acquired Time	4/23/2015 11:29:35 AM				



ESI-MS spectrum of compound 2

BIT2015-002 in DMSO-d6
A.R.No : NE15D014

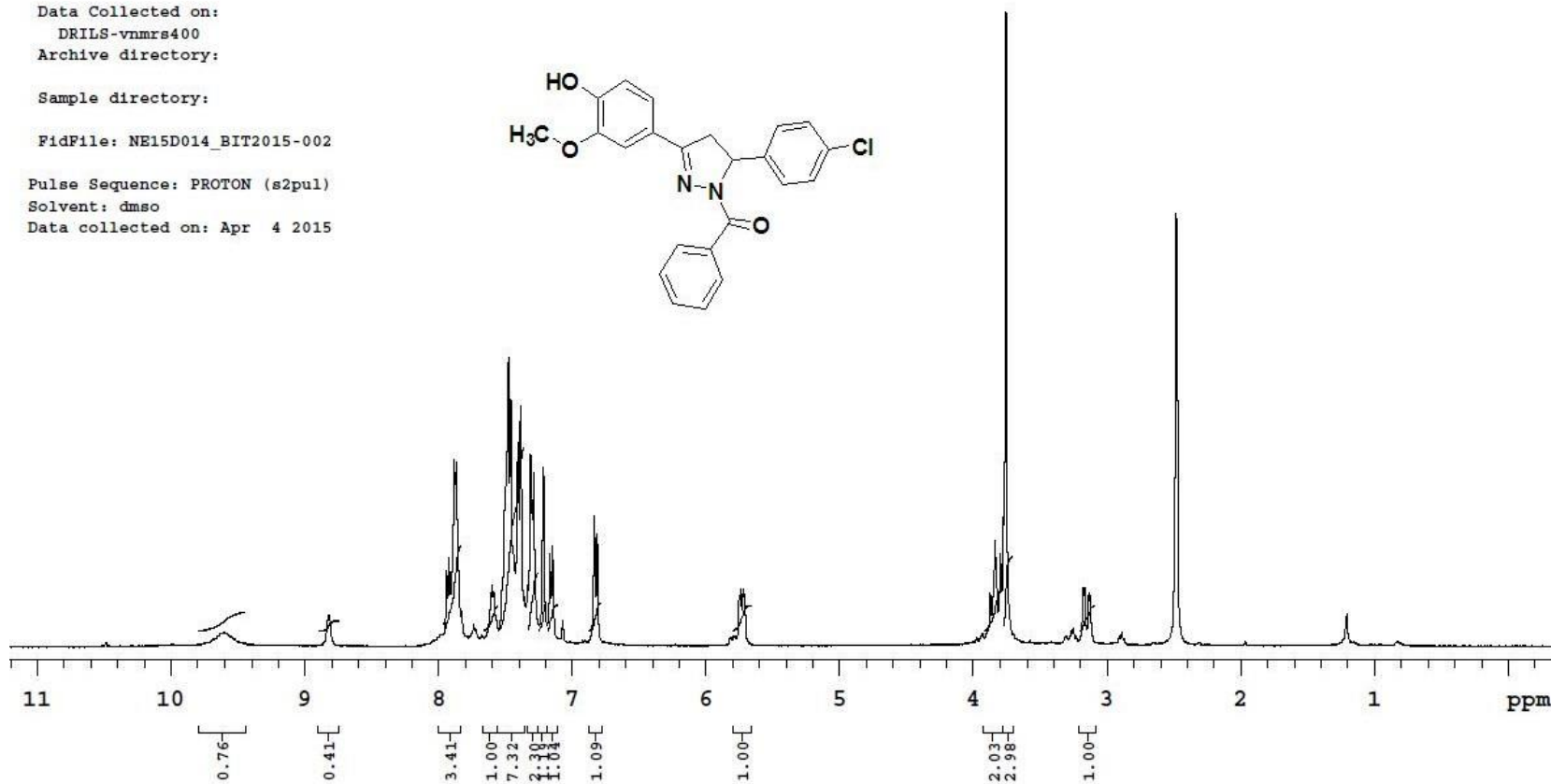
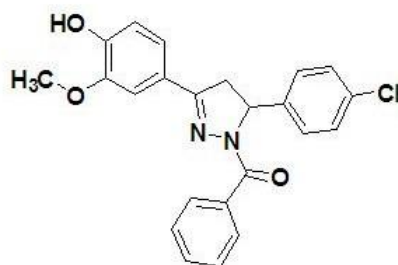
Sample Name:

Data Collected on:
DRILS-vnmrs400
Archive directory:

Sample directory:

FidFile: NE15D014_BIT2015-002

Pulse Sequence: PROTON (s2pul)
Solvent: dmso
Data collected on: Apr 4 2015



¹H-NMR (400 MHz, DMSO-d₆) spectrum of compound 3

Sample Name BIT2015-002

Position

Vial 19

Sample type

Instrument Name

Instrument 1

User Name

Inj Vol

0.5

Data Filename

230415M019.d

ACQ Method

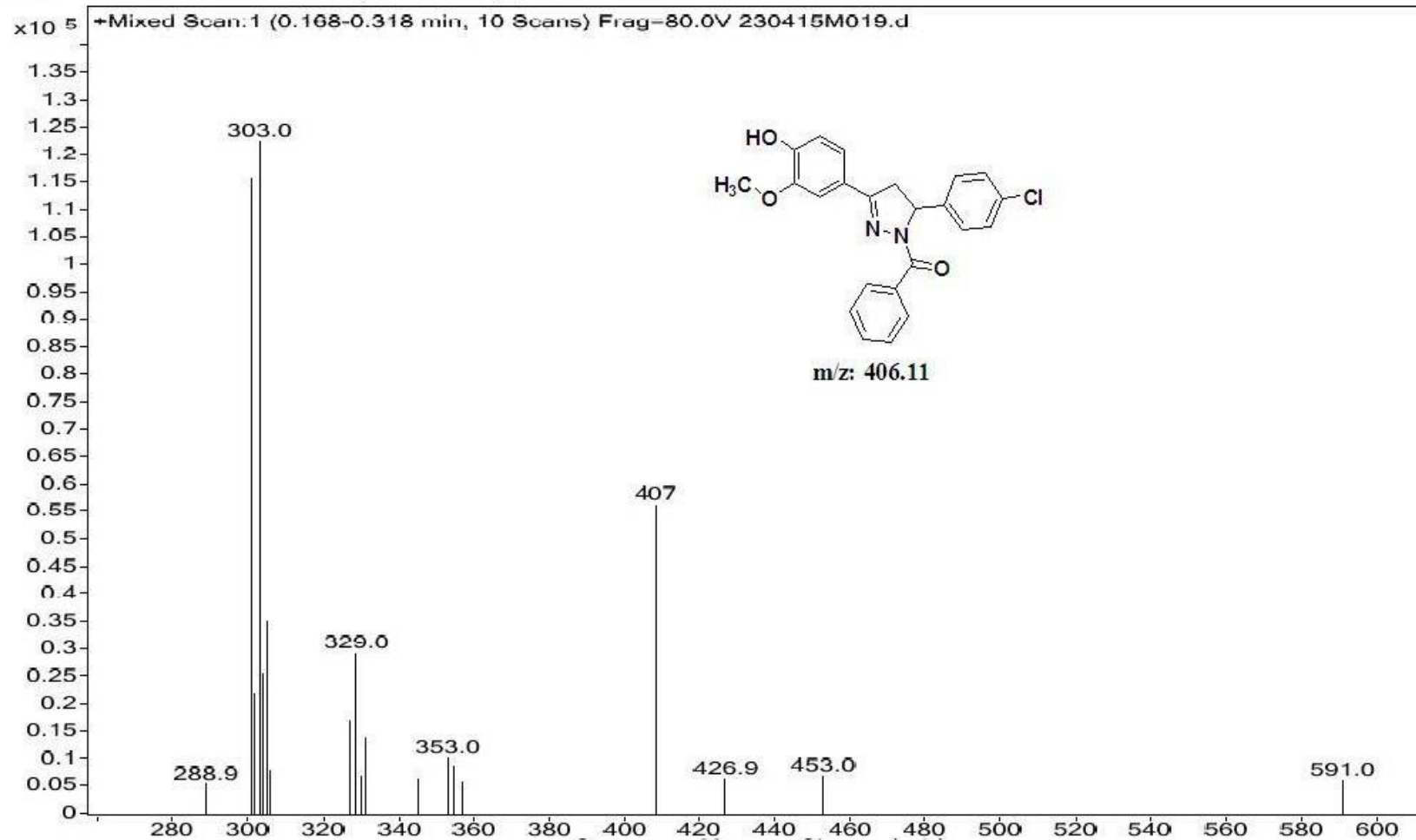
test.m

AR NO :

ME15D096

Acquired Time

4/23/2015 11:30:47 AM



ESI-MS spectrum of compound 3

BIT2015-004 in DMSO-d6
A.R.No : NE15F001

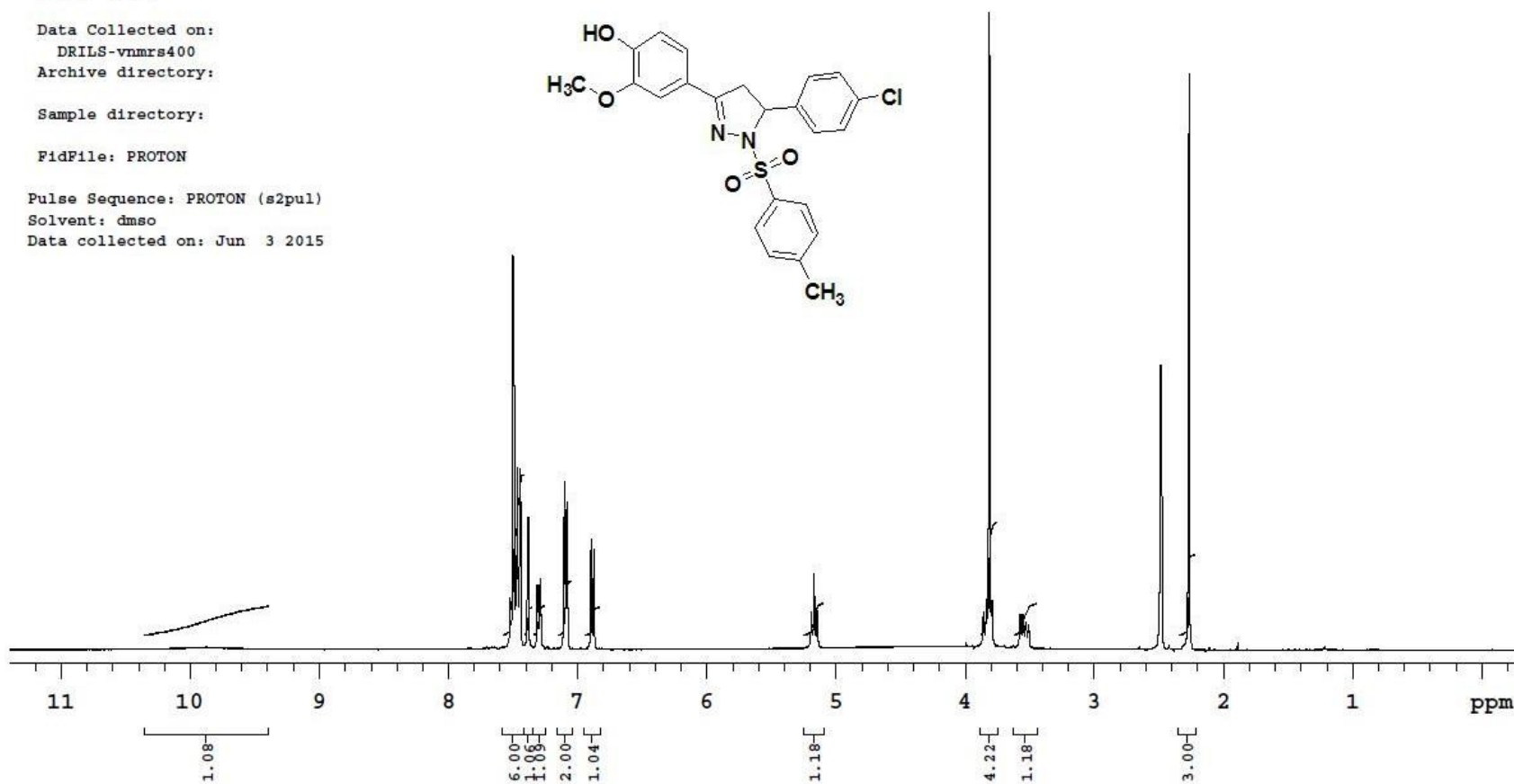
Sample Name:

Data Collected on:
DRILS-vnmrs400
Archive directory:

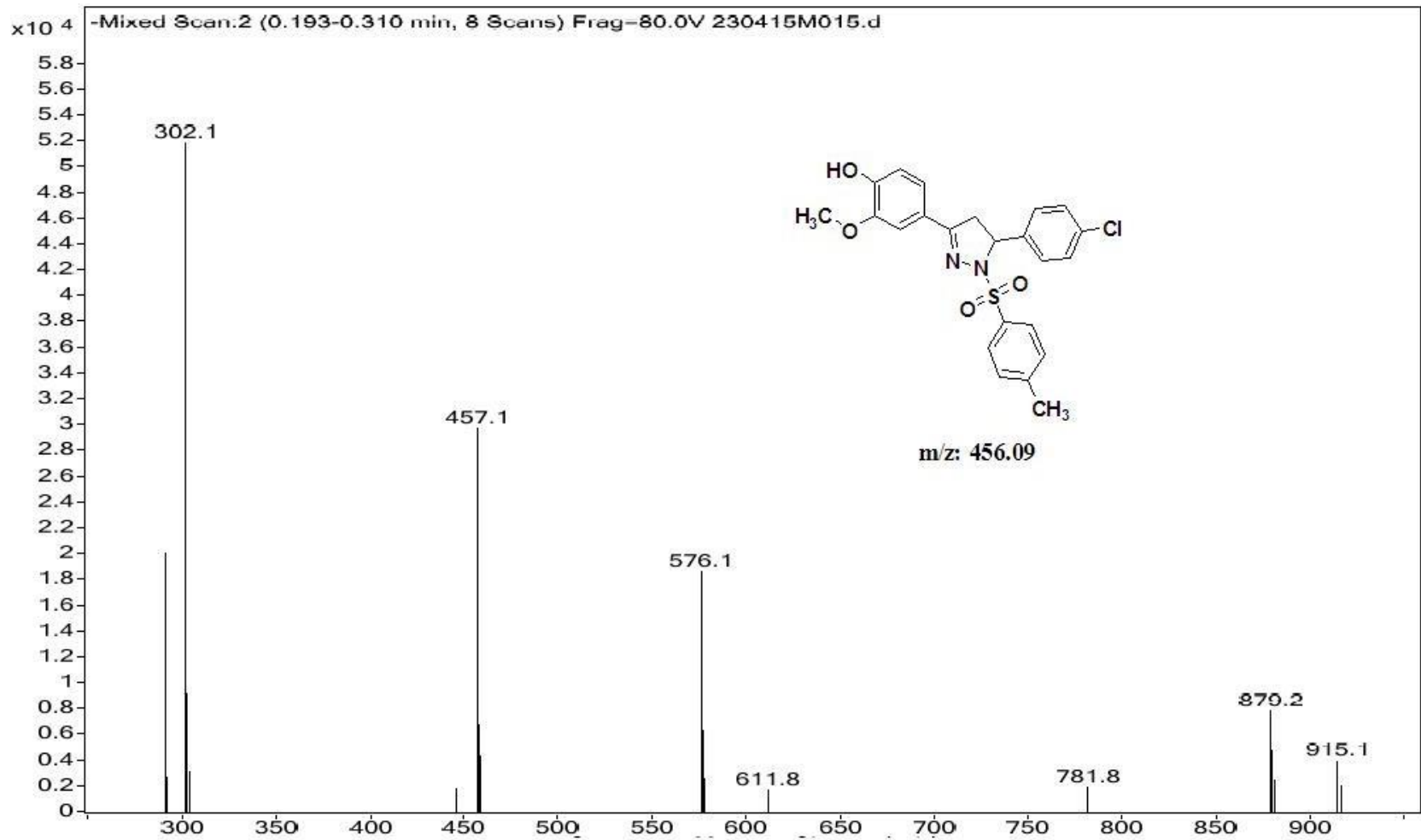
Sample directory:

FidFile: PROTON

Pulse Sequence: PROTON (s2pul)
Solvent: dmsc
Data collected on: Jun 3 2015



¹H-NMR (400 MHz, DMSO-d₆) spectrum of compound 4



ESI-MS spectrum of compound 4

BIT2015-004 in DMSO-d6

13C EXPT.

A.R.NO: NE15F002

Sample Name:

Data Collected on:

DRILS-vnmrs400

Archive directory:

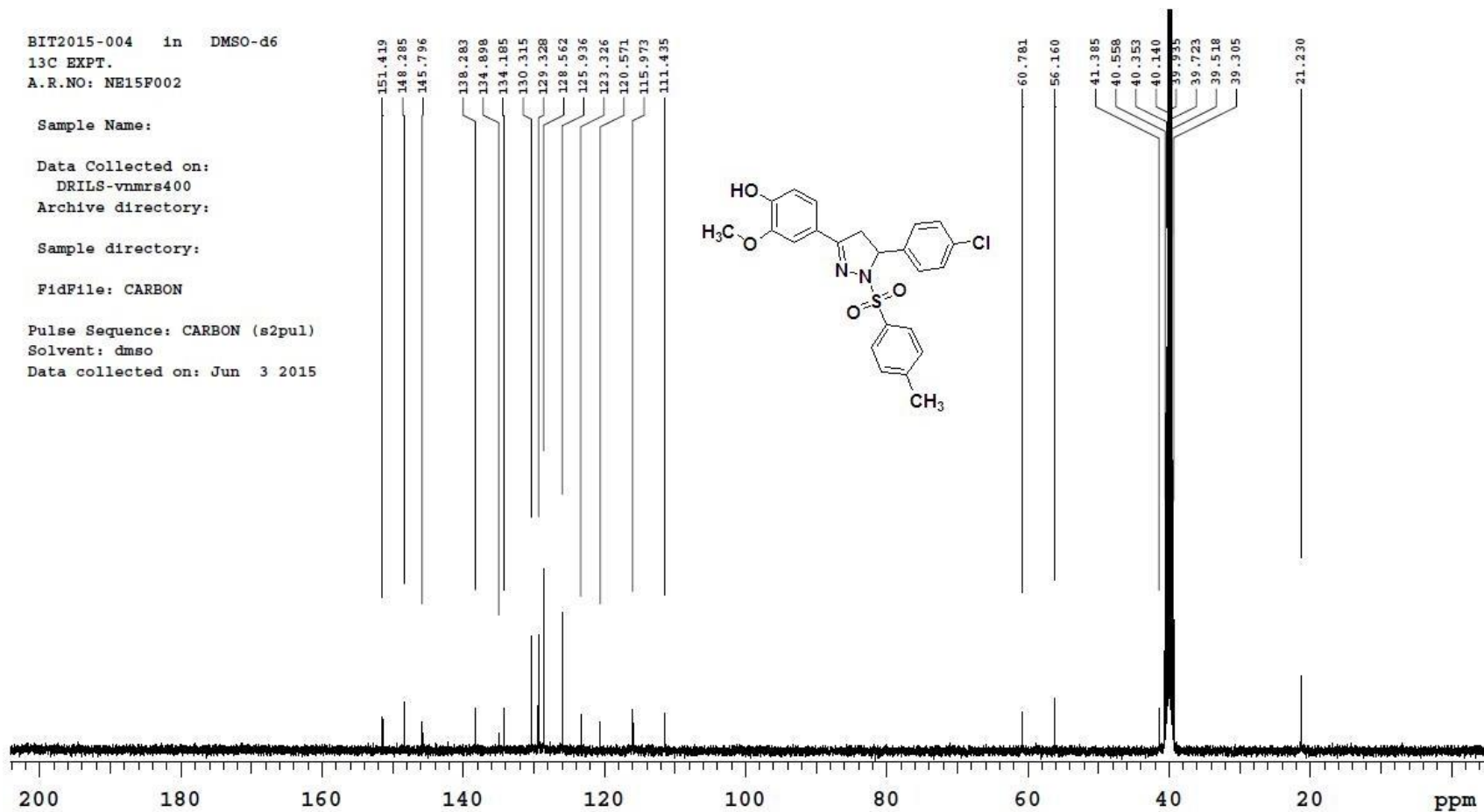
Sample directory:

FidFile: CARBON

Pulse Sequence: CARBON (s2pul)

Solvent: dmsd

Data collected on: Jun 3 2015



¹³C-NMR (100 MHz, DMSO-d₆) spectrum of compound 4

BIT2015-006 in DMSO-d6
A.R.No : NE15D018

Sample Name:

Data Collected on:

DRILS-vnmrs400

Archive directory:

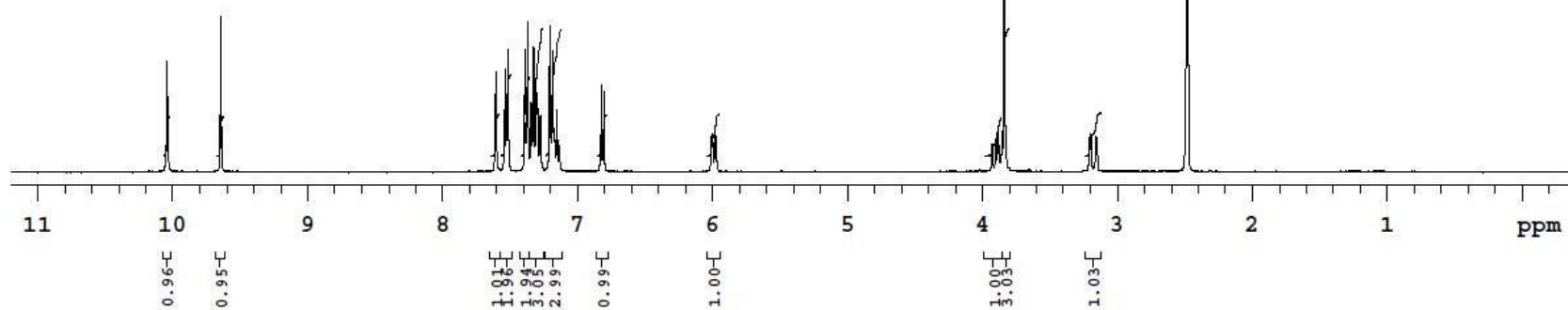
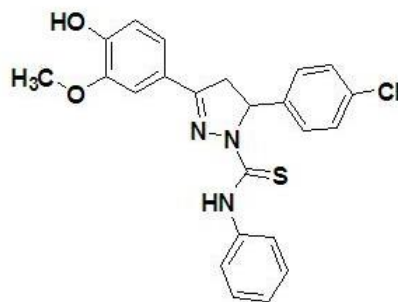
Sample directory:

FidFile: NE15D018_BIT2015-006

Pulse Sequence: PROTON (s2pul)

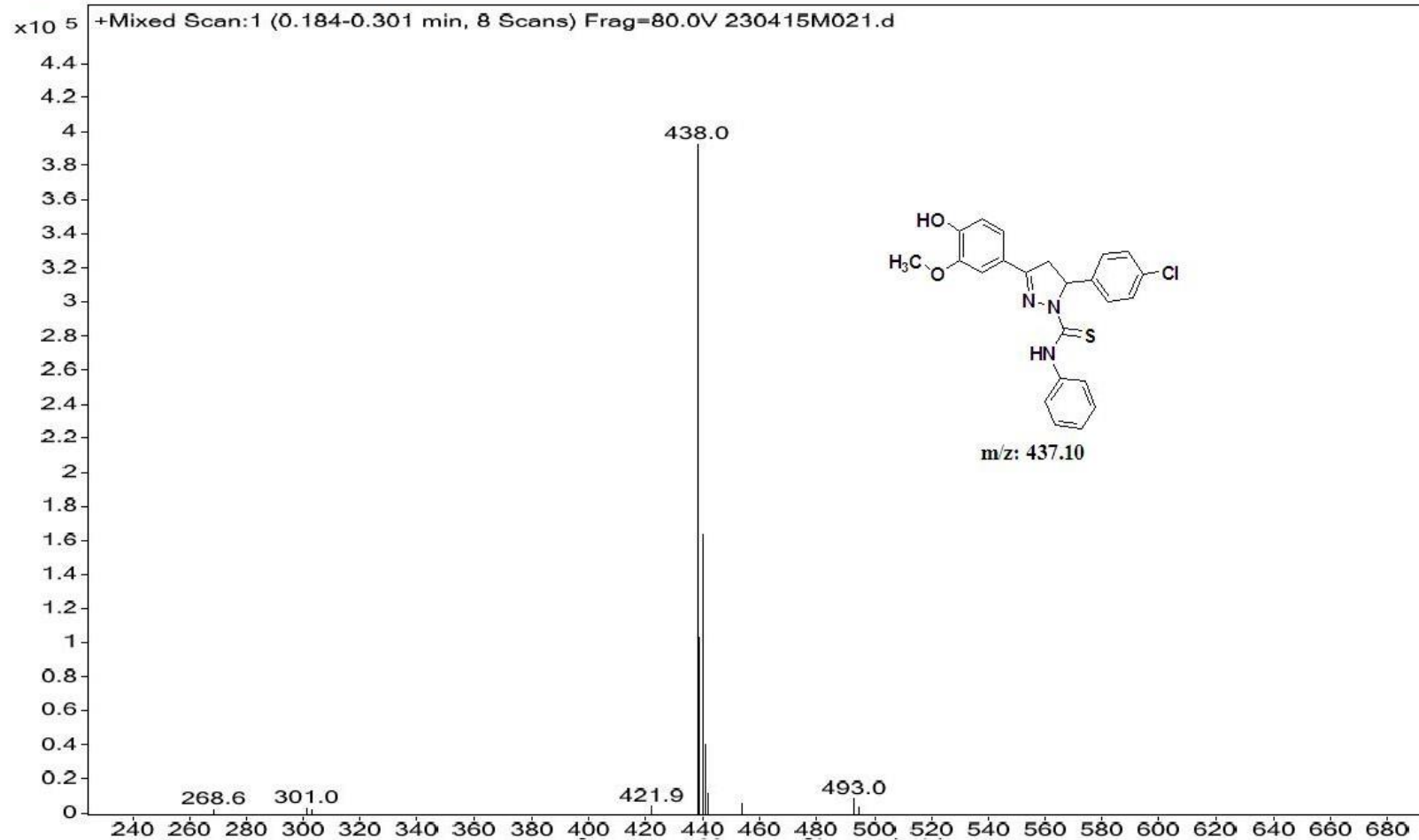
Solvent: dmso

Data collected on: Apr 4 2015



¹H-NMR (400 MHz, DMSO-d₆) spectrum of compound 5

Sample Name	BIT2015-006	Position	Vial 21	Sample type		Instrument Name	Instrument 1
User Name		Inj Vol	0.5	Data Filename	230415M021.d	ACQ Method	test.m
AR NO :	ME15D098	Acquired Time	4/23/2015 11:33:15 AM				



ESI-MS spectrum of compound 5

BIT2015-005 in DMSO-d6
A.R.No : NE15D017

Sample Name:

Data Collected on:

DRILS-vnmrs400

Archive directory:

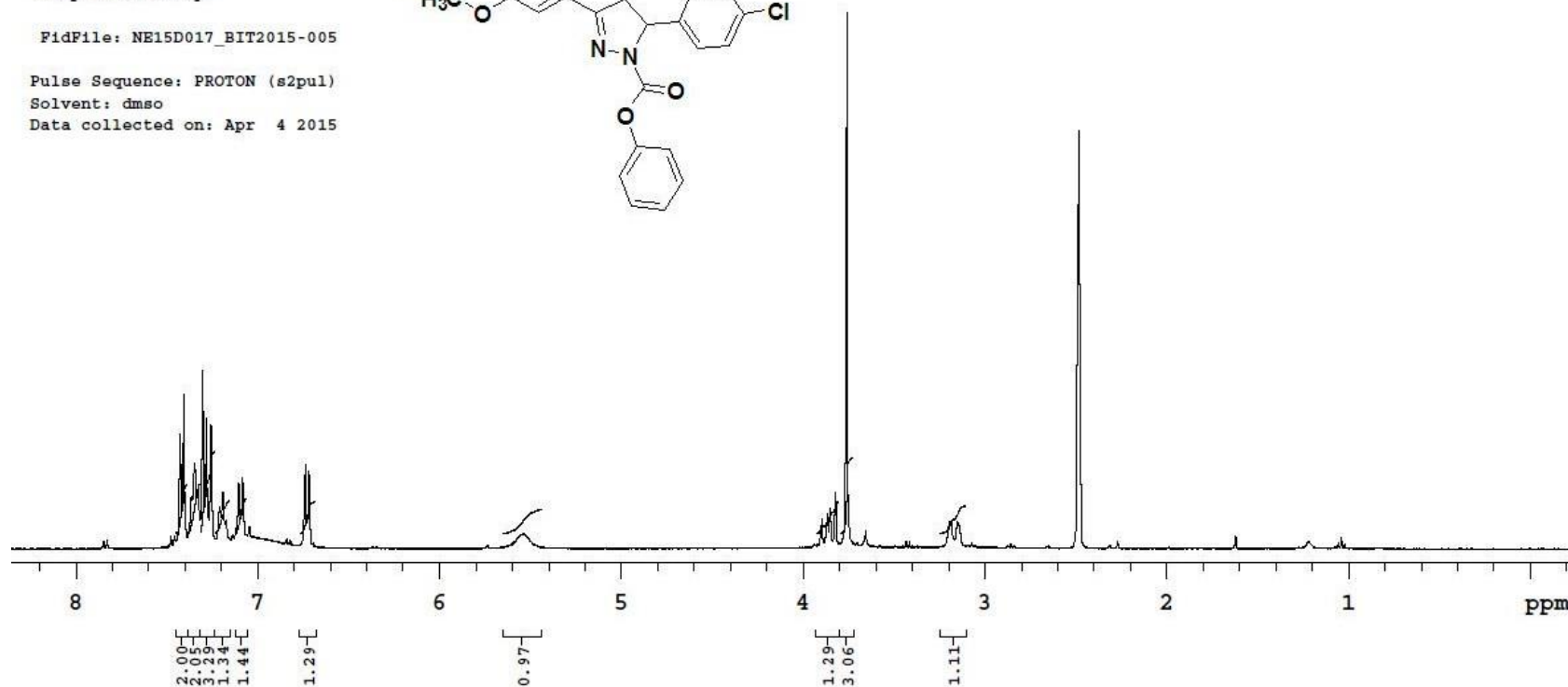
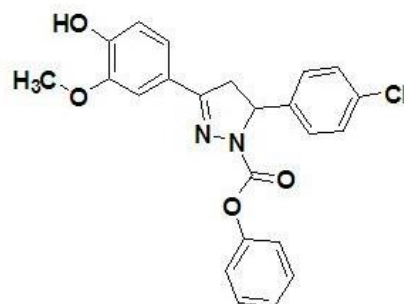
Sample directory:

FidFile: NE15D017_BIT2015-005

Pulse Sequence: PROTON (s2pul)

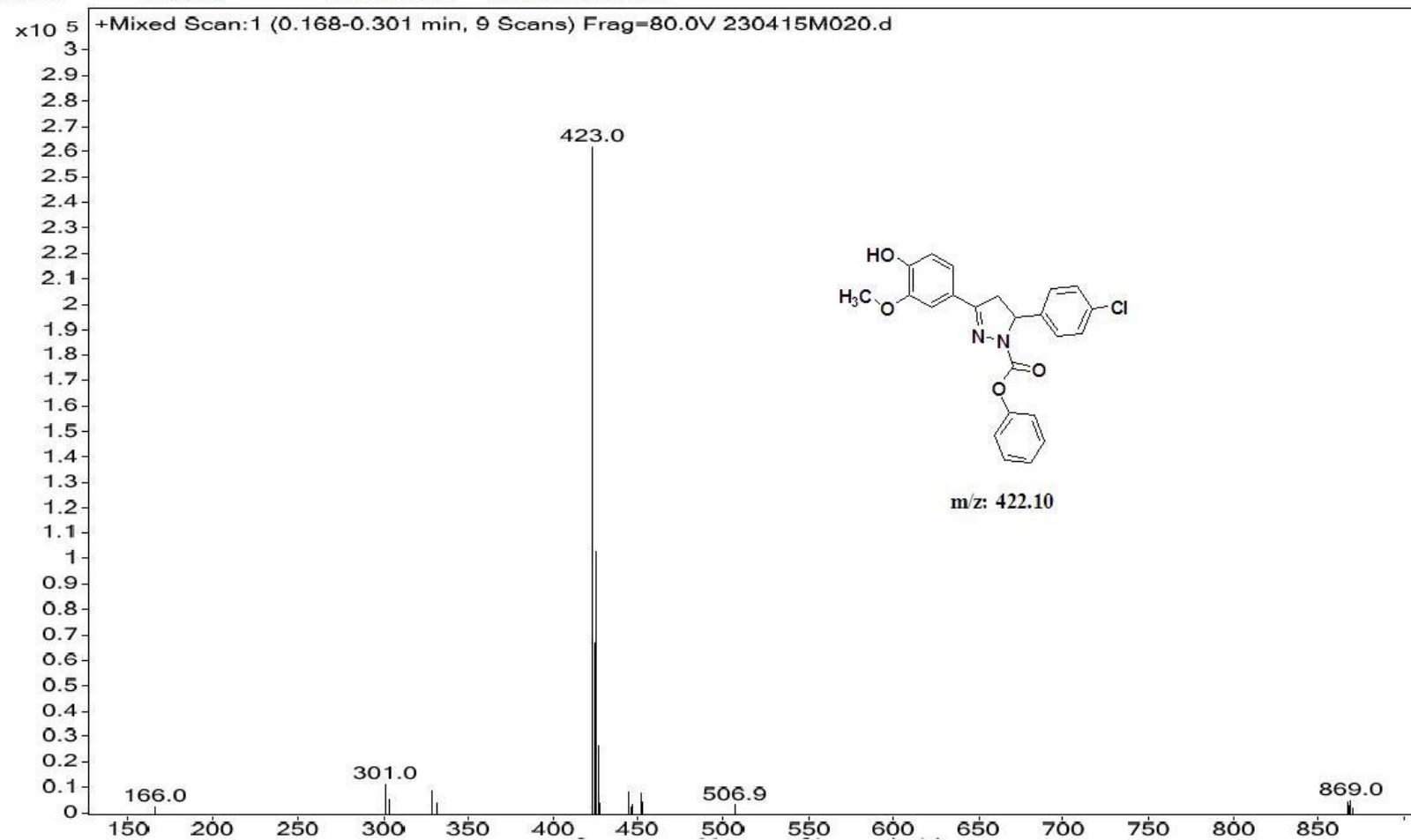
Solvent: dms

Data collected on: Apr 4 2015

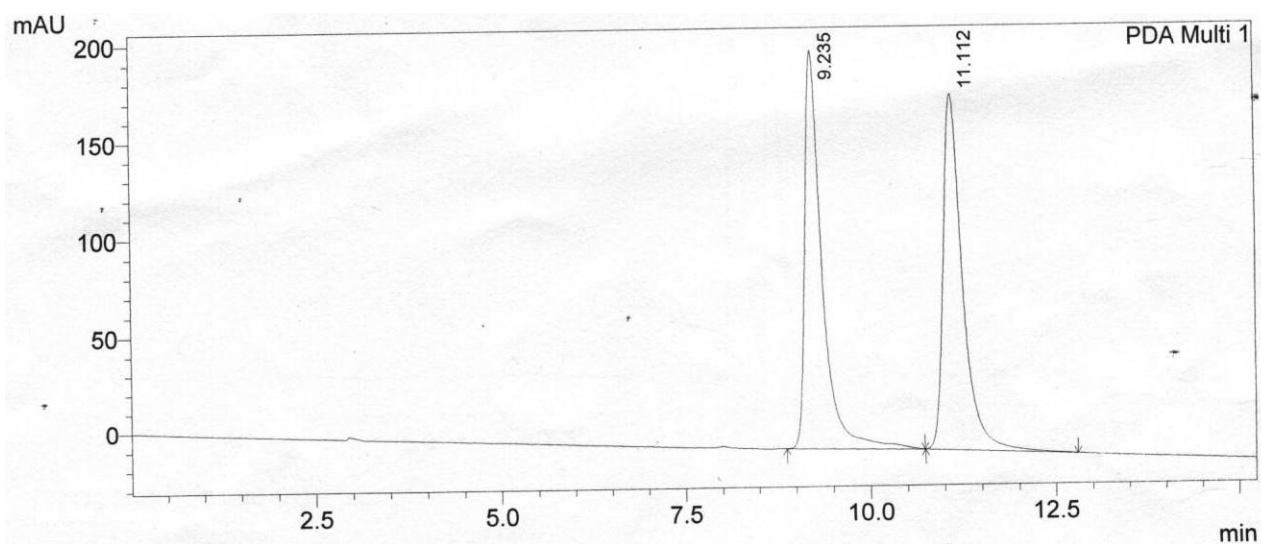


¹H-NMR (400 MHz, DMSO-d₆) spectrum of compound 6

Sample Name	BIT2015-005	Position	Vial 20	Sample type		Instrument Name	Instrument 1
User Name		Inj Vol	0.5	Data Filename	230415M020.d	ACQ Method	test.m
AR NO :	ME15D097	Acquired Time	4/23/2015 11:32:01 AM				



ESI-MS spectrum of compound 6



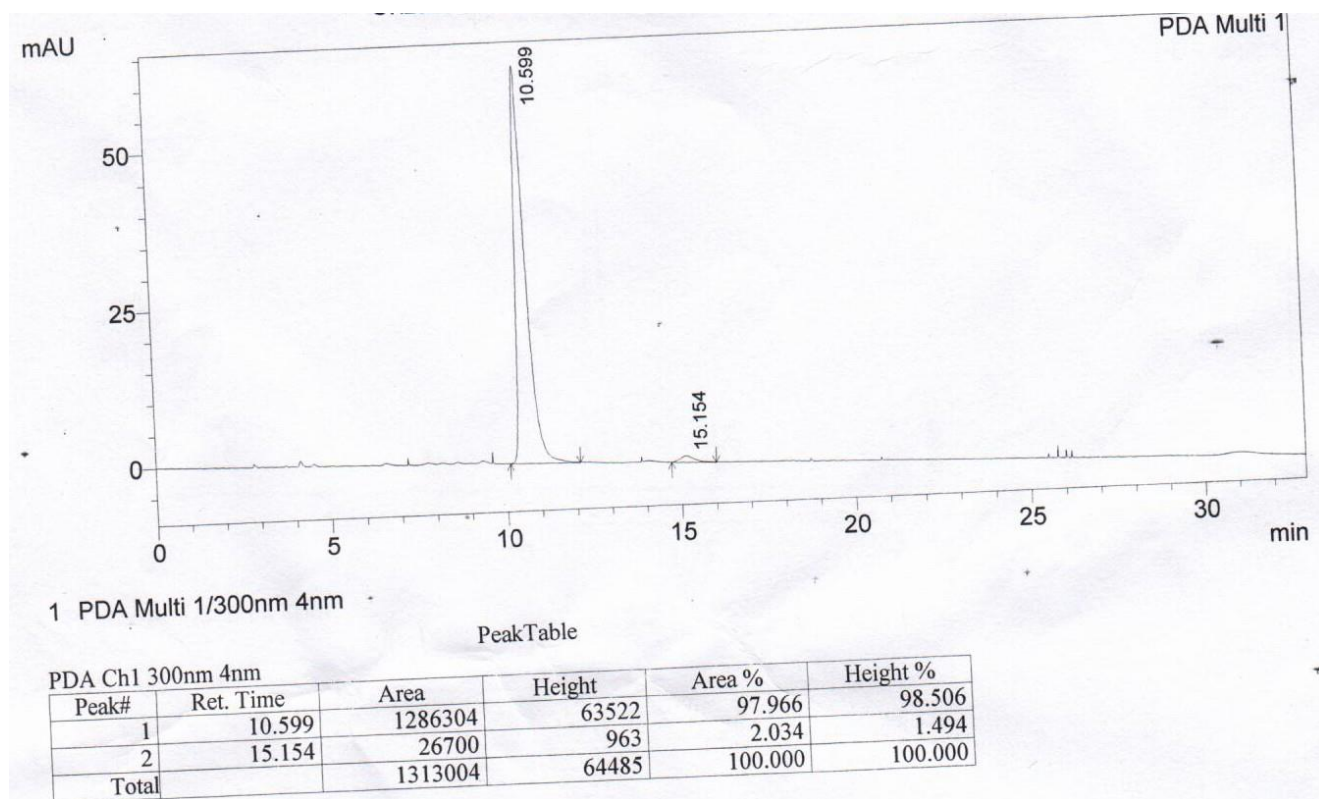
1 PDA Multi 1/301nm 4nm

PeakTable

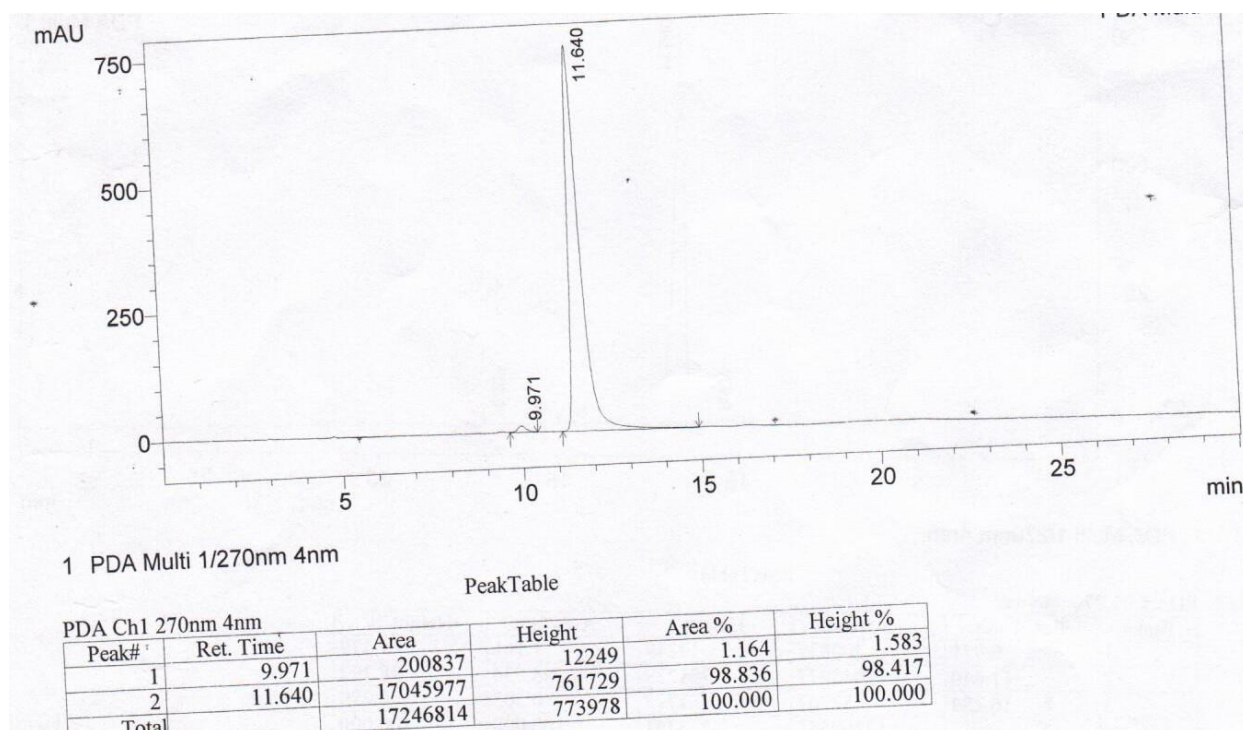
PDA Ch1 301nm 4nm

Peak#	Ret. Time	Area	Height	Area %	Height %
1	9.235	3310400	205855	49.996	52.757
2	11.112	3310897	184336	50.004	47.243
Total		6621297	390192	100.000	100.000

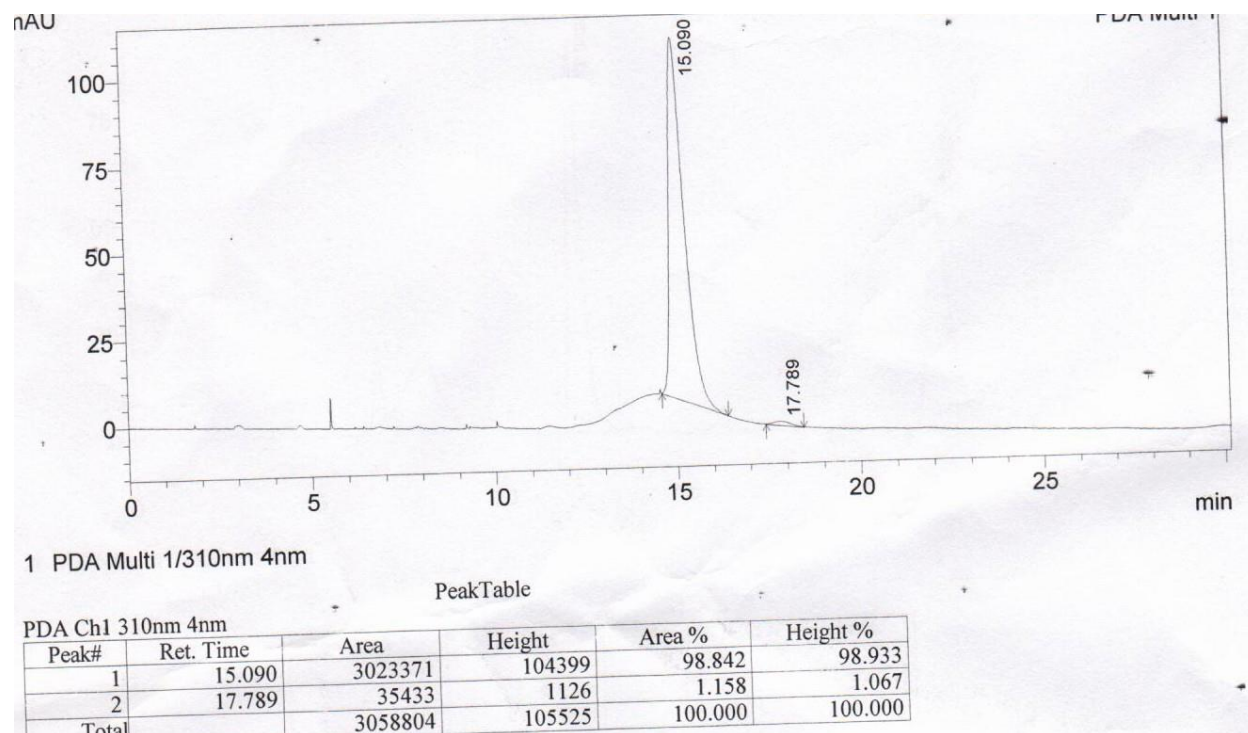
Compound 2: Mobile Phase: 5% Isopropyl alcohol in Hexane



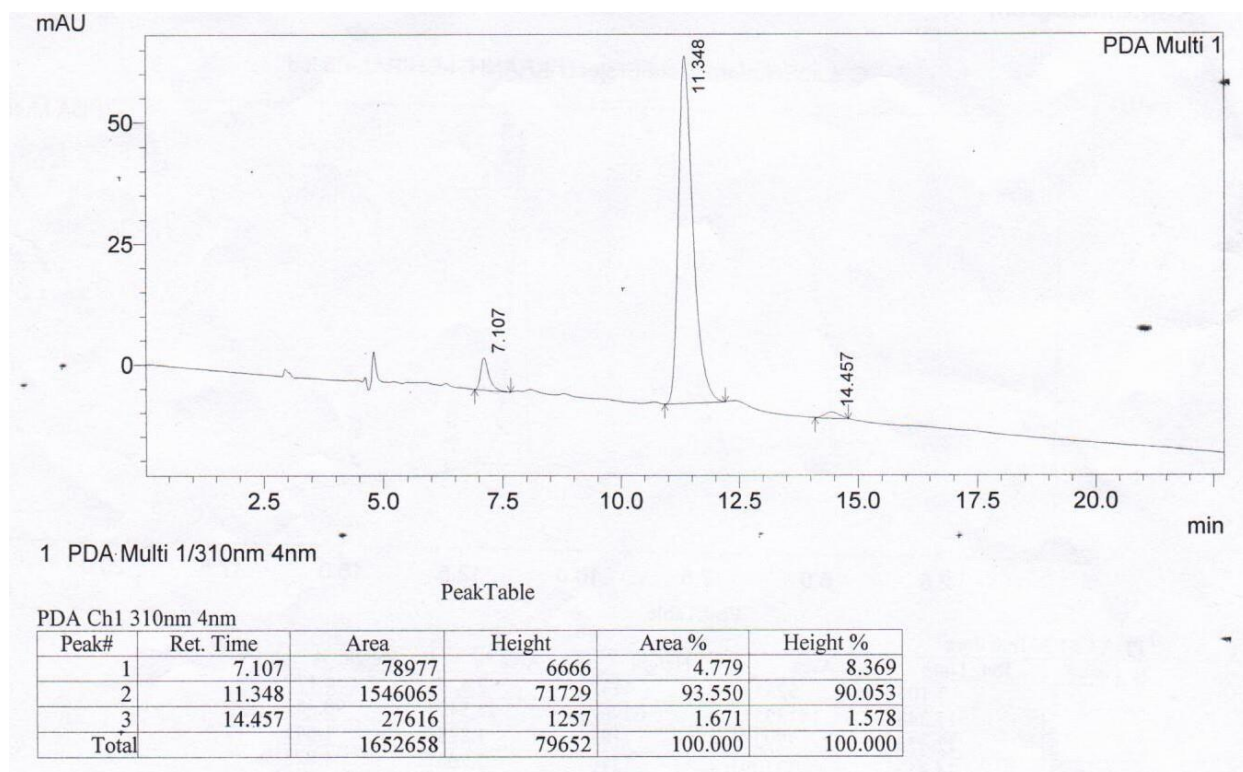
Compound 3: Mobile Phase: 10% Isopropyl alcohol in Hexane



Compound 4: Mobile Phase: 5% Isopropyl alcohol in Hexane



Compound 5: Mobile Phase: 10% Isopropyl alcohol in Hexane



Compound 6: Mobile Phase: 5% Isopropyl alcohol in Hexane

References

1. Sahoo, A.; Yabanoglu, S.; Sinha, B. N.; Ucar, G.; Basu, A.; Jayaprakash, V., Towards development of selective and reversible pyrazoline based MAO-inhibitors: Synthesis, biological evaluation and docking studies. *Bioorganic & medicinal chemistry letters* **2010**, *20* (1), 132-136.
2. Jagrat, M.; Behera, J.; Yabanoglu, S.; Ercan, A.; Ucar, G.; Sinha, B. N.; Sankaran, V.; Basu, A.; Jayaprakash, V., Pyrazoline based MAO inhibitors: synthesis, biological evaluation and SAR studies. *Bioorganic & medicinal chemistry letters* **2011**, *21* (14), 4296-4300.
3. Nayak, B. V.; Ciftci-Yabanoglu, S.; Jadav, S. S.; Jagrat, M.; Sinha, B. N.; Ucar, G.; Jayaprakash, V., Monoamine oxidase inhibitory activity of 3, 5-biaryl-4, 5-dihydro-1H-pyrazole-1-carboxylate derivatives. *European journal of medicinal chemistry* **2013**, *69*, 762-767.
4. Bradford, M. M., A rapid and sensitive method for the quantitation of microgram quantities of protein utilizing the principle of protein-dye binding. *Analytical biochemistry* **1976**, *72* (1-2), 248-254.
5. Chimenti, F.; Carradori, S.; Secci, D.; Bolasco, A.; Bizzarri, B.; Chimenti, P.; Granese, A.; Yanez, M.; Orallo, F., Synthesis and inhibitory activity against human monoamine oxidase of N1-thiocarbamoyl-3, 5-di (hetero) aryl-4, 5-dihydro-(1H)-pyrazole derivatives. *European journal of medicinal chemistry* **2010**, *45* (2), 800-804.
6. Hansen, M. B.; Nielsen, S. E.; Berg, K., Re-examination and further development of a precise and rapid dye method for measuring cell growth/cell kill. *Journal of immunological methods* **1989**, *119* (2), 203-210.
7. Wu, C. F.; Bertorelli, R.; Sacconi, M.; Pepeu, G.; Consolo, S., Decrease of brain acetylcholine release in aging freely-moving rats detected by microdialysis. *Neurobiology of aging* **1988**, *9*, 357-361.
8. Di, L.; Kerns, E. H.; Fan, K.; McConnell, O. J.; Carter, G. T., High throughput artificial membrane permeability assay for blood-brain barrier. *European journal of medicinal chemistry* **2003**, *38* (3), 223-232.
9. Son, S. Y.; Ma, J.; Kondou, Y.; Yoshimura, M.; Yamashita, E.; Tsukihara, T., Structure of human monoamine oxidase A at 2.2-Å resolution: the control of opening the entry for substrates/inhibitors. *Proceedings of the National Academy of Sciences of the United States of America* **2008**, *105* (15), 5739-44.
10. Ravindranath, P. A.; Forli, S.; Goodsell, D. S.; Olson, A. J.; Sanner, M. F., AutoDockFR: Advances in Protein-Ligand Docking with Explicitly Specified Binding Site Flexibility. *PLoS computational biology* **2015**, *11* (12), e1004586.
11. Harris, R.; Olson, A. J.; Goodsell, D. S., Automated prediction of ligand-binding sites in proteins. *Proteins* **2008**, *70* (4), 1506-17.
12. Kollman, P. A.; Massova, I.; Reyes, C.; Kuhn, B.; Huo, S.; Chong, L.; Lee, M.; Lee, T.; Duan, Y.; Wang, W.; Donini, O.; Cieplak, P.; Srinivasan, J.; Case, D. A.; Cheatham, T. E., 3rd, Calculating structures and free energies of complex molecules: combining molecular mechanics and continuum models. *Accounts of chemical research* **2000**, *33* (12), 889-97.